LAWRENCE
LIVERMORE
NATIONAL
LABORATORY

UCRL-CONF-222509

APPLICATION OF THE EMBEDDED FIBER OPTIC PROBE IN HIGH EXPLOSIVE DETONATION STUDIES: PBX-9502 AND LX-17

D.E. Hare, D.R. Goosman, K.T. Lorenz, E.L. Lee

September 27, 2006

13th International Detonation Symposium
Norfolk, VA, United States
July 23, 2006 through July 28, 2006

APPLICATION OF THE EMBEDDED FIBER OPTIC PROBE IN HIGH EXPLOSIVE DETONATION STUDIES: PBX-9502 AND LX-17

UCRL-CONF-222509

D. E. Hare, D. R. Goosman, K. Thomas Lorenz, and E. L. Lee

Lawrence Livermore National Laboratory
Livermore, CA 94551

Abstract. The Embedded Fiber Optic probe directly measures detonation speed continuously in time, without the need to numerically differentiate data, and is a new tool for measuring time-dependent as well as steady detonation speed to high accuracy. It consists of a custom-design optical fiber probe embedded in high explosive. The explosive is detonated and a refractive index discontinuity is produced in the probe at the location of the detonation front by the compression of the detonation. Because this index-jump tracks the detonation front a measurement of the Doppler shift of laser light reflected from the jump makes it possible to continuously measure detonation velocity with high spatial and temporal resolution. We have employed this probe with a Fabry-Perot-type laser Doppler velocimetry system additionally equipped with a special filter for reducing the level of non-Doppler shifted light relative to the signal. This is necessary because the index-jump signal is relatively weak compared to the return expected from a well-prepared surface in the more traditional and familiar example of material interface velocimetry.

Our observations were carried out on a number of explosives but this work is focused on our results on PBX-9502 (95% TATB, 5% Kel-F) and LX-17 (92.5% TATB, 7.5% Kel-F) at varying initial charge density. Our measurements reveal a density dependence significantly lower than previous quoted values and lower than theoretical calculations. Our limited data on detonation speed dependence on wave curvature is in reasonable agreement with previous work using more standard methods and confirms deviation from the Wood-Kirkwood theoretical formula.

INTRODUCTION

We have taken advantage of the capabilities of a new experimental technique, the Embedded Fiber Optic (EFO) probe, to make continuous high resolution measurements of the time-dependent evolution in detonation speed in long columns (L/D = 6) of LX-17 and PBX-9502 as well as the dependence of this process on initial density.

The generally accepted but not well documented value for the dependence of detonation speed on density for LX-17 and PBX-9502 is 3.0 mm/μs per g/cc. The EFO probe afforded the opportunity to confirm or correct this dependence at a cylindrical charge diameter of 25.4 mm simply by performing tests at different charge densities.

Our value for $dD/d\rho_0$ for LX-17 of 2.489 (+/- 0.01) mm/μs per g/cc and for PBX-9502 of 2.62

mm/μs per g/cc derived from our observations is somewhat lower than the aforementioned "accepted" value of this quantity. Because the reaction zone length in TATB compositions is known to be rather large we can't discount the possibility that this value might still approach 3.0 in the plane wave limit.

The Embedded Fiber Optic (EFO) technique is relatively new and was developed by D.R. Goosman and his group.[1] This report is not intended to be a detailed discussion of the EFO equipment and technique. However, we give a brief synopsis of EFO.

The EFO technique utilizes laser Doppler velocimetry to measure *wave* speed (detonation speed or shock speed) continuously in time. The EFO technique for measuring detonation speed involves embedding a custom-made fiber optic probe (the EFO probe) within a detonating explosive. Figure 1 illustrates the basic principles involved.

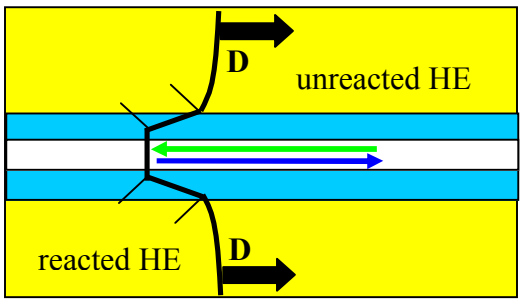

Figure 1. The basics of the EFO process. In the region close to the probe the detonation in the surrounding explosive forms and maintains a shock wave in the probe. It is the latter that reflects and Doppler-shifts light: thus what the velocimeter actually measures is the instantaneous velocity of the shock wave in the fiber. The fiber shock wave velocity versus time (velocity history) often very closely follows the detonation speed history of the surrounding explosive although some care needs to be taken to correct the data for the response function of the probe when the velocity is changing very rapidly in time. Note the probe core is grossly enlarged relative to the cladding for illustrative clarity.

Because the refractive index-jump at the shock interface is small, the desired Doppler-shifted intensity is weaker by roughly a factor of 30 relative to the un-Doppler-shifted reflections which naturally occur due to static scattering imperfections in the velocimetry system. In order to obtain quality EFO data in our Fabry-Perot velocimetry system[2] we additionally need to use a special filter system which preferentially rejects the non-Doppler shifted component relative to the EFO signal. This special filter is a dedicated separate Fabry-Perot interferometer that acts as a filter to reject the non-Doppler shifted component while preserving the Doppler shifted component thus greatly improving the ratio of Doppler to non-Doppler shifted signal that shows up at the streak camera detection system. The details of our special filter[3] and our Fabry-Perot velocimetry system[2] are discussed elsewhere.

The probe is a custom multi-mode fiber with a thick cladding of poly-tetrafluoroethylene (PTFE) and a narrow core of aqueous CsCl solution. This assembly acts like a total-internal-reflection waveguide for the 532 nm light and additionally has a very low sound speed, lower than any detonation speed we may wish to measure. This latter condition is required in order for the reflective interface within the EFO probe to be hydrodynamically stable and thus enables the interface to form and track the detonation correctly.

EXPERIMENTAL PREPARATIONS

All the booster and main charge pellets were hot ram pressed in-house from PBX-9407 (the booster: 94% RDX, 6% Exon 461), PBX-9502, and LX-17 molding powders. A special pressing plunger with a central steel pin was custom constructed to press the 1.00 inch diameter pellets with the 0.160 cm hole needed for the EFO probe. Thus no drilling of the HE pellets was necessary to perform these experiments.

All four shots were cylindrically symmetric (barring small deviations such as the narrow slot in the polycarbonate outer tube wall) and hence can be reasonably modeled by using a 2-D hydrocode. An RP-1 exploding bridge wire detonator (EBW) is used to initiate the PBX-9407 booster. The RP-1 is manufactured by RISI (Reynolds Industry Systems Incorporated, San Ramon, CA) and the reader is referred to the manufacturer's data literature for the fine details of this detonator. The EFO probe is made from PTFE

tubing of 1.60 mm O.D. with a tiny I.D. of 175 μm that is injected with filtered, nearly saturated aqueous CsCl solution (solution index of refraction at 25 ^{0}C and 532 nm wavelength is typically 1.411). For hydrodynamic simulation purposes we model the probe as a solid rod of PTFE of 1.60 mm diameter since the overwhelming majority of the probe is the PTFE cladding.

Our measured density is the average for the pellet mass / volume with the volume measured as the cylinder length and the diameter taken at orthogonal positions and averaged, accounting for the probe hole.

The shots were assembled as a vertical column on a shot stand with the RP-1 and booster on the bottom. The boosters were all nominally 25.4 mm diameter by 12.7 mm thick PBX-9407 pressed to a nominal 1.6 g/cc. The pellets were greased / wrung together and the small annular gap (order 20 μm) between the EFO probe and the charge was stemmed with water to give more intimate probe-HE contact. The probe extended the entire length of the main charge and the booster, all the way down to the face of the RP-1. To give the shot some structural integrity the column was assembled in a thin polycarbonate tube of 1.50 mm wall thickness. This tube results in a slight increase in confinement which we discuss later.

Ram-pressed pellets are known to have density gradient issues. We did not radiographically quantify these density gradients but we did orient every pellet so that the side of the pellet that had been in contact with the moving plunger during the pressing operation faced away from the detonator for all pellets, boosters included, on all shots. This would tend to orient any pressing-induced density gradient so that the density (and thus the detonation speed) would increase as the detonation progressed within an isolated pellet.

TABLE 1. Material information for our four shots. Booster was PBX-9407 all cases.

Shot #	main chg	Avg ρ0 of column	booster avg ρ0
170	LX-17	1.880 g/cc	1.621 g/cc
171	LX-17	1.809	1.619
198	PBX-9502	1.899	1.613
199	PBX-9502	1.800	1.621

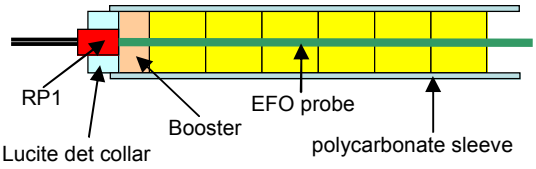

FIGURE 2. geometry of our four shots: The column is 25.4 mm diameter, composed of a 12.7 mm long booster followed by the main charge of six 25.4 mm long pellets. Main charge has L/D of 6:1. The probe goes all the way to the face of the RP1.

RESULTS

Our velocimetry system records on custom designed streak cameras. The fringe record is recorded on hard film, then digitized on a special negative scanner. Figure 3 is a good example of a resulting velocimetry record. Our system is a two-cavity system. The reference cavity fringes eliminate any velocity ambiguity issue.

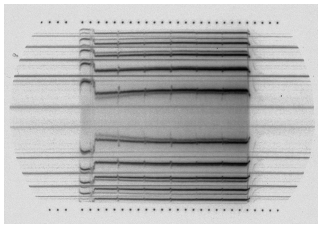

FIGURE 3. Fabry-Perot record of shot 198. Note the position fiducials naturally formed by the grease junctions between the six pellets of the main charge (the vertical blips in the Doppler shifted fringes that show up at regular time intervals). The time dots are spaced at 1 μs intervals.

The digitized records were analyzed both by hand, and using a data reduction program developed by G.R. Avara[4]. The apparent velocity obtained directly from the fringe analysis must be multiplied by 1.0014 (corrects for finite numerical aperture of the velocimeter)[1] and divided by the index of refraction of the EFO probe core. This latter correction may not be familiar to users that are otherwise familiar with standard laser Doppler velocimetry techniques and is discussed in reference 1. Although it is generally more difficult to work with liquid core probes, it is relatively easy to measure the core index of refraction of such a probe using a standard refractometer. The CsCl

core index of refraction is typically about 1.411 at 532 nm and 24 ^{0}C and can be readily measured to a few parts in 10,000.

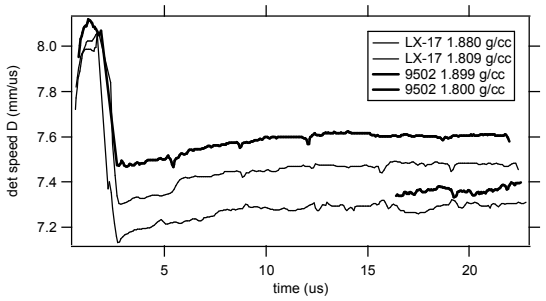

FIGURE 4. Velocity versus time plots for all four experiments. The booster signal also shows up and is the higher velocity plateau at the far left. LX-17 is the lighter trace. The respective lower density shots are the lower final velocity traces. The lower density 9502 record is only partial, the consequence of a probe defect.

Figure 4 displays the four detonation speed histories. Two for LX-17 (shots 170 and 171) and two for PBX-9502 (shots 198 and 199). Unfortunately we lost the record for all but the final two pellets of shot 199, probably due to a bubble that nucleated in the probe after assembly. Nevertheless the short record of 199 still yields useful information about steady detonation in PBX-9502 and $dD/d\rho_0$. For the higher density LX-17 shot the first pellet of the column had a significantly lower density than the rest of the pellets in the column (by about 1 %) and this shows up very clearly in the velocity history (2 to 5.5 μs).

Although the HE pellets were carefully greased together and these joints are only on the order of a few microns thick they often show up very clearly in the velocity history as sharp negative spikes. These sharp spikes actually form useful position fiducials and can be used to perform a self-consistency test of our ability to measure detonation speed. (They also give an indication of the time response of the probe).

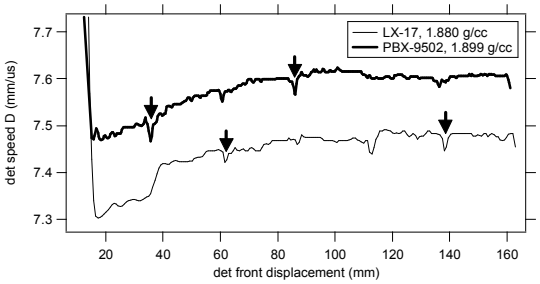

FIGURE 5. The integration test: A good self-consistency check. PBX-9502 thick line: velocity integrated on time = 50.33 mm, pellet lengths added = 50.71 mm. LX-17 thin line: velocity integrated on time = 76.57 mm, pellet lengths added = 76.51 mm. The arrows show the start and end positions where this test was carried out. The lower value of D in the first pellet of the LX-17 column is due to its lower density relative to the rest of the column. Note that time, the natural independent variable in our measurements, is easily converted to detonation front displacement by simply integrating D with respect to time.

The test (Fig. 5) is to compare the time integral of the detonation speed between two grease-junction fiducials to the sum of the recorded lengths of the pellets between the two fiducials (measured during assembly). If the velocity data reduction was not done correctly these two results will not be equal. For example: If one did not know to divide the apparent velocity by the probe core refractive index then the length obtained by integrating D in time would be 41% greater than the measured length from the assembly data.

Shot 199, the partial PBX-9502 record at 1.802 g/cc, displays interesting behavior that is reminiscent of density gradients from the ram pressing. Note how D rises within the next-to-last pellet as the detonation goes through it, drops abruptly at the grease junction (about 19.3 μs) and then rises again as it goes through the final pellet.

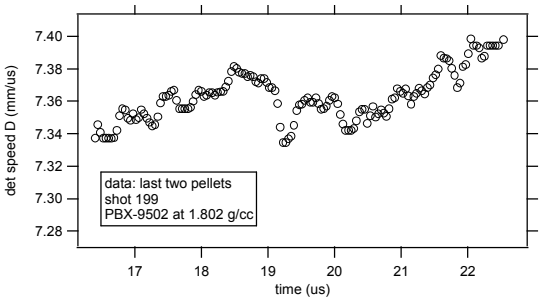

FIGURE 6. detail of shot 199. The gradient in D suggests a gradient of 0.4% in density across the length of a pellet (25.4 mm).

DISCUSSION

The three full-record-length shots show that the detonation speed has become effectively constant by the end of the third pellet in each column. The time-dependent behavior is suggestive of exponential relaxation of an initial perturbation to a time-independent, or steady state, and so we fit the full length main charge records to:

$$D = D_0 + A\exp\left(-\left(\frac{z - z_0}{\alpha}\right)\right) \qquad (1)$$

This formula should be taken as an empirical expedient. We make no claim to a theoretical basis for it. Note that D_0 is not the plane wave limit, but the steady speed for our geometry (25.4 mm diameter charges). The amplitude of the perturbation A is a negative number for our experiments as our RP-1 / booster system always initiates the main charge with more curvature (and hence starts out at a lower value of D) than what the steady detonation state requires. However this will not be universally the case. For example, plane wave initiation of a long column would give a positive value for A.

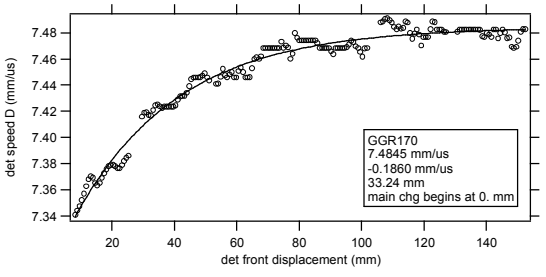

FIGURE 7. data of shot 170 fit to the exponential relaxation form. D of the first pellet has been corrected for its low density relative to the remainder of the column. We used the curve fitting routine from IGOR Pro (WaveMetrics, Inc, Lake Oswego, OR) for this and all the fits related to this work.

These fits do two things for us: They give a nice consistent value for D_0 and a characteristic length that allows us to quantify how many charge diameters the detonation needs to run to attain steady velocity characteristic of the charge diameter.

To attempt an answer to how the probe might affect this measurement we simulated shot 170 using the CALE 2-D hydrocode[5] and the Tarver ignition and growth model of LX-17 without modification.[6-8]

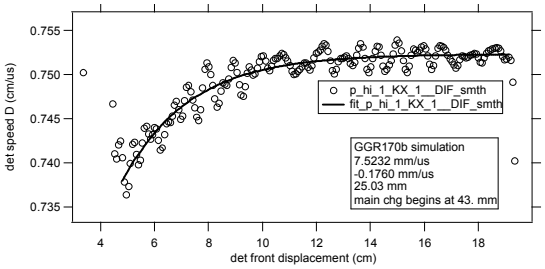

FIGURE 8. exponential form fit to CALE simulation. circles are simulation output, line is the fit to that output.

TABLE 2. Eq. 1 exponential fits to the data and simulations. "d" is charge diameter and $dD/d\rho_0$ is at constant charge diameter of 25.4 mm

Shot ident.	α (mm)	α/d (dimless)	D_0 (mm/μs)	$dD/d\rho_0$
170	33.24	1.31	7.4845	2.489
171	25.11	0.99	7.2968	"
198	28.40	1.12	7.6121	2.62
199			7.37	"
Simulate 170				
With probe	25.03	0.98	7.5232	
Without probe	26.71	1.05	7.5382	

The simulations indicate that for our 25.4 mm diameter charge geometry the presence of the

fiber had a negligible effect on the rate of evolution towards D_0, although it does reduce the steady detonation speed by 0.23 %.

Our values of $dD/d\rho_0$ are strictly speaking only valid for constant diameter of 25.4 mm. They are considerably lower than values previously quoted in the literature.[9,10] Campbell and Engelke refer to the value 3 mm/μs per g/cc in a footnote (not 3.0, but 3) and state that "The value of this coefficient is only known at large stick diameter." Bahl et al refer to 3.94 which we believe may have come from a thermochemical calculation. It is not impossible that the value of $dD/d\rho_0$ may actually be 3 or greater at infinite diameter and yet consistent with our findings. We find very modest qualitative support for this scenario in our LX-17 data. They support a value slightly lower (10%) if the first pellets in the column, which have greater front curvature and hence would logically correspond to smaller diameter, are used to estimate $dD/d\rho_0$ instead of the final pellets.

We compare our steady detonation speed results to previous work using more conventional time-of-arrival detectors and long columns. To make these comparisons it is necessary to make slight corrections, typically sub-1%, for density difference, difference in confinement, and the presence of the fiber in our shot. We correct for density using our values of $dD/d\rho_0$ found in this work. The corrections for fiber and confinement difference were made by simulating our shot 170 using the CALE hydrocode[5] and the ignition and growth reactive flow model for LX-17.[6-8] We used these simulations to quantify the effect of the presence / absence of the probe and the effect of changes in confinement on steady detonation speed.

Souers and Garza performed an extensive series of detonation speed measurements in long columns of LX-17 using time-of-arrival pins.[11] They have two shots in 25.4 mm diameter columns with length-to-diameter greater than 13 at 1.890 g/cc and they measure 7.515 mm/μs. When our LX-17 result is compensated for density difference (using our value of $dD/d\rho_0$), for our slightly more effective confinement (-0.06%, estimated from simulation), and the presence of the fiber in our shot (+0.23%, estimated from simulation) we get 7.520 mm/μs for our result, a difference of 0.06%.

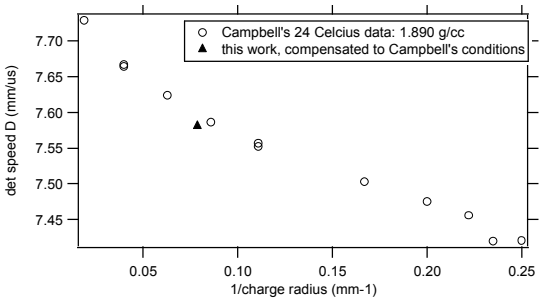

FIGURE 9. Our PBX-9502 steady data point shown on Campbell's data [11] adjusted to his density and confinement conditions.

We can also compare our PBX-9502 data to that of Campbell.[12] Our result is shown in Fig. 9 compensated for density, for the fiber (+0.23%), and for the confinement difference (-0.29%). Our result, adjusted to his conditions, is lower by about 0.3%.

The EFO technique can measure steady detonation speed to sub-1% accuracy, but as we have seen it also has the ability to track continuous time-dependent detonation speed without the need to numerically differentiate the output. However, time-dependent measurements require a little more caution in interpretation. The probe has a characteristic time response that must be considered. There are three aspects to the response: 1) A short time delay: It takes a time on the order of 100 ns for the interior of the probe to know of any changes in the exterior driving conditions. 2) a convolution-like smoothing action 3) A velocity decrement or increment related to the time-dependent change in the shape (particularly the depth) of the reflective interface as a function of the pressure driving the probe. The first is present in both time-dependent and independent flow, but doesn't really have an impact on time-independent measurements. The other two concern only time-dependent measurements.

A detailed analysis of this response function is important but beyond the scope of the current work. However we know that these issues are not problems in our current discussion and analysis because regarding issue two: we restrict ourselves to discuss time-dependent behavior that is slow compared to the fiber response time, and regarding issue three: the range of pressure driving conditions in these experiments is relatively narrow.

Our data and our simulations support the empirical single exponential evolution to the steady detonation speed as a reasonable description of the data behavior. It is very nearly simply exp(-z/d) where d is the charge diameter. We suggest the possibility that this result might be more universal and might hold to good approximation for most cylindrical explosive charges independent of the explosive as long as it is above failure and goes completely to the steady state. After the detonation has propagated 3 diameters our empirical relationship reduces the original perturbation or velocity decrement to exp(-3) or 5% of its original value. This means that if for example the detonation speed was originally 10% below the steady value then it should climb to within 0.5% of the steady value after propagating 3 charge diameters.

Although our experiments were really not designed to measure front radius of curvature S dependence of D, we can make some statements about D versus S. The front radius of curvature has been measured on the exit surface of an RP-1 / PBX-9407 booster system very similar to the one we use.[13] The radius of curvature of the wavefront on the booster output surface was measured to be S = 20 (+/-) 1 mm. The paraxial refractive correction to the radius of curvature due to the difference in detonation speed between booster and main charge is given by $S_2 = S_1 * D_1/D_2$ and adds about 2 mm to S. This implies that the initial value of S as it first enters our main charge is about S = 22 mm.

Before the detonation near the axis/probe location has had time to communicate with the side release, we might expect the radius of curvature of the wavefront to evolve in a very simple way with respect to the front displacement: For at least a short amount of time it should grow as a simple spherically expanding wave with a fixed center. For our systems this would give S = 22 mm + z, where z is the location of the detonation front relative to the end of the booster / beginning of the main charge. However we know that this simple spherical expansion can't proceed indefinitely as S must asymptotically approach the finite value dictated by a 25.4 mm diameter column. Our data indicate that this is mostly complete by the end of the third pellet. Given the above considerations we chose to remap the data of only our first 1.5 pellets from D versus z to D versus 1/S space using the spherical expansion S, z relationship.

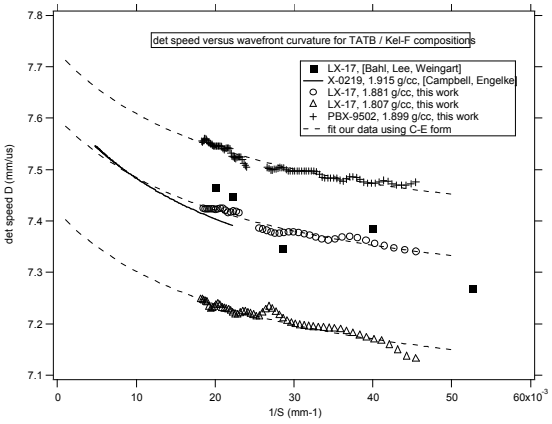

FIGURE 10. Our data in D vs 1/S space plotted against spherical expansion in LX-17 hemispheres from Bahl, Lee, and Weingart, and the Campbell-Engelke fit (over the range of their data) to their D versus S data in X-0219 (90 % TATB, 10 % Kel-F).

The well-known Wood-Kirkwood relationship relating D to S is:[14]

$$D = D_\infty \left(1 - \frac{\alpha}{S} \right) \qquad (2)$$

α is the reaction zone length multiplied by a dimensionless constant on the order of 3. Wood-Kirkwood is a straight line in D versus 1/S space. Our data do not fit Wood-Kirkwood in a logically satisfactory manner, giving values for D_∞ which are clearly too low to be correct.

The Campbell-Engelke form improves upon the Wood-Kirkwood formula by allowing for a reaction zone length which can decrease with decreasing S.[9] They showed that a simplified version of their general expression worked well for TATB compostions. This simplified form, which we will refer to simply as the C-E form, is given by:

$$D = D_\infty \left(1 - \frac{BA}{\left(S - A' \right)} \right) \qquad (3)$$

A Taylor series expansion of the C-E form in 1/S shows that the product BA is first order and is interpreted to be the reaction zone length at

infinite diameter and A' influences second and all higher orders (Note: we will follow the Campbell-Engelke parameter nomenclature and sign convention with A' = -41 (+/-7) mm for X-0219). A' determines how the reaction zone length changes with S.

Our data are insufficient to perform a fully unconstrained fit of C-E in which D_∞, BA, and A' are all allowed to vary. However we believe there is some limited use to be had from fitting this data since D_∞ will be rather difficult and expensive to measure. We decided to accept the value of the A' coefficient from the Campbell-Engelke work on X-0219 as a reasonable estimate, and the resultant constrained fits are also plotted as the dashed lines in Fig 10. The parameters from the fits are listed in Table 3.

TABLE 3. Fit coefficents: comparison of the C-E form fits[8] of X-0219 and this work.

data set	D_∞ (mm/μs)	AB (mm)	A' (mm)
X-0219, 1.915 g/cc	7.627 +/- 0.015	2.66 +/- 0.4	-41 +/- 7
LX-17, 1.881 g/cc	7.601 +/- 0.008	2.15 +/- 0.1	Fixed -41
LX-17, 1.807 g/cc	7.418 +/- 0.009	2.20 +/- 0.1	Fixed -41
PBX-9502, 1.899 g/cc	7.728 +/- 0.005	2.18 +/- 0.05	Fixed -41

It is interesting that the fitted parameter AB was virtually the same for all our results and about 20 % lower than the value Campbell and Engelke obtained for X-0219. In hindsight an equal or better choice might have been to fix AB to the Campbell-Engelke value of 2.66 rather than fixing A'. Had we chosen to do this the fitted values of D_∞ would have been slightly higher. However our data are not sufficient in range and accuracy to warrant a more exhaustive fitting effort. We do point out that if we form the difference quotient between our two LX-17 data C-E fits at 1/S = 0 we arrive at an estimate for $dD/d\rho_0$ at infinite diameter of 2.47 mm/μs per g/cc: interesting in that it is very close to our 25.4 mm diameter value. However given the extrapolations and assumptions used to arrive at this value, it must be considered tentative.

As a final consideration we come back to the time evolution of D. A very simple picture of the evolution of the curvature is that it expands spherically right up to the point it reaches the required asymptotic curvature and then remains at that value for all later times. What would this simple process look like relative to our data? In Fig 11 we have overlayed our shot 170 data with the above-described process, generated with the help of our C-E form fit on the same data. Recall that this fit was performed using data only from the first 1.5 pellet-lengths of the column.

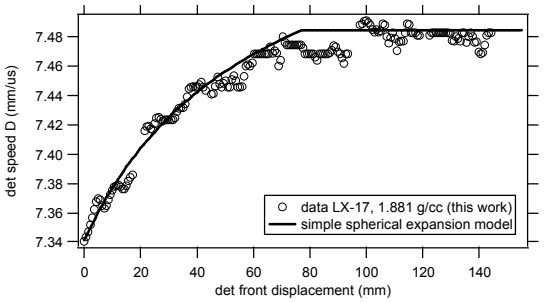

FIGURE 11. shot 170 data against simple spherical expansion model.

The overlay is not so bad, although not as good in the transition region as the exponential description. The attractive point of the spherical model is that it should be a physically correct description for the initial evolution of detonation speed in the case of point source initiation of a long column. A hybrid between the two models might capture the best features of both, but we have not attempted it in this paper.

ACKNOWLEDGEMENTS

This work could not have been accomplished without a lot of expert and professional help from many talented individuals: From Lawrence Livermore National Laboratory: Sally R. Weber for pressing all of the pellets, Denise A. Grimsley for operation of the Fabry-Perot velocimeter and streak camera system, James T. Wade as the optical technologist and laser operator, Kou Moua for fabricating the shot hardware, Brian A. Cracchiola and Rich Villafanna for explosives handling and firing operator support, and Bradley M. Wong, Estes Vincent, and Robert P. (Bob) Hall for electronic technical support. Andrew Hernandez for photographic support and for heading-up construction of the special HE pellet pressing components. Chadd M. May made us

aware of important data on the RP-1. P.C. Souers and Raul G. Garza shared their LX-17 result with us in pre-published form. Raul together with Jeffrey Chandler did our HE assembly, handling, and ramrod work. Dan Phillips performed critical booster breakout wavefront radius of curvature measurements. Jon Price of RISI helped us in further understanding some of the RP-1 specifications and data. G. Rex Avara (retired, formerly LLNL) wrote the velocimetry data reduction software and assisted us in its utilization. Finally, in memory of Kurt Sinz for his initial inspiration and support in pursuing this investigation.

This work was performed under the auspices of the U.S. Department of Energy by University of California, Lawrence Livermore National Laboratory under Contract W-7405-Eng-48.

REFERENCES

1. D.R. Goosman, J.T. Wade, R.G. Garza, G.R. Avara, T.R. Crabtree, A.T. Rivera, D.E. Hare, D.R. Tolar Jr., B.A. Bratton, "Optical probes for continuous Fabry-Perot velocimetry inside materials", 26th International Congress on High-Speed Photography and Photonics. Edited by Paisley, Dennis L.; Kleinfelder, Stuart; Snyder, Donald R.; Thompson, Brian J. Proceedings of the SPIE, Volume 5580, pp. 517-528 (2005).

2. D. Goosman, G. Avara, L. Steinmetz, C. Lai, S. Perry, Lawrence Livermore National Laboratory report: UCRL-JC-123809, 1996.

3. David Goosman, George Avara, James Wade, and Anthony Rivera, Lawrence Livermore National Laboratory report: UCRL-JC-145646-REV-1, 2002.

4. G. Avara, Lawrence Livermore National Laboratory report: UCRL-ID-145355, 2001.

5. R.E. Tipton, unpublished result.

6. E.L. Lee and C.M. Tarver, "Phenomenological Model of Shock Initiation in Heterogeneous Explosives', Phys.Fluids**.23**(12) pp 2362-2372, 1980

7. C.M. Tarver, J.O. Hallquist, and L.M. Erickson, "Modeling short pulse duration shock initiation of solid explosives", 8th International Detonation Symposium, Albuquerque, NM, USA (1985)

8. L.G. Green, C.M. Tarver, D.J. Erskine, "Reaction Zone Structure in Supracompressed Detonating Explosives", Proceedings Ninth Symposium (International) on Detonation, Portland, OR, August 28-Sept 1, 1989, p.670 (1989)

9. A.W. Campbell and R. Engelke, The Diameter Effect in High Density Heterogeneous Explosives", Sixth Symposium on Detonation, pp 642- 652, 1976

10. K.L.Bahl, R.S.Lee, and R.C.Weingart, " Velocity of Spherically Diverging Detonation Waves," Shock Waves in Condensed Matter, pp 559-562, 1984

11. P.C. Souers and R.G. Garza, private communication.

12. A. W. Campbell, "Diameter Effect and Failure Diameter of a TATB Based Explosive", Propellants, Explosives, and Pyrotechnics, pp183-187,(1984)

13. K. Thomas Lorenz and Dan F. Phillips, unpublished result.

14. W.W. Wood and J.G. Kirkwood, "Diameter Effect in Condensed Explosives" J. Chem. Phys, **22**,(11) p 1920, 1954